Twin Lossy Mode Resonance (LMR) on a single D-shaped optical fiber

J.J. IMAS,[1,2,*] C. R. ZAMARREÑO,[1,2] P. ZUBIATE,[1] I. DEL VILLAR,[1,2] J.M. PÉREZ-ESCUDERO,[3] I.R. MATÍAS[2]

[1] *Electrical, Electronic and Communications Engineering Department, Public University of Navarra, 31006 Pamplona, Spain*
[2] *Institute of Smart Cities (ISC), Public University of Navarra, 31006 Pamplona, Spain*
[3] *Antenna Group, Public University of Navarra, 31006 Pamplona, Spain*
**Corresponding author: josejavier.imas@unavarra.es*

Received XX Month XXXX; revised XX Month, XXXX; accepted XX Month XXXX; posted XX Month XXXX (Doc. ID XXXXX); published XX Month XXXX

This Letter presents the fabrication of dual lossy mode resonance (LMR) refractometers based on titanium dioxide (TiO_2) and tin dioxide (SnO_2) thin films deposited on a single side-polished D-shaped optical fiber. For the first time, two independent LMRs are obtained in the same D-shaped optical fiber, by using a step shaped nanostructure consisting of a first section of TiO_2 with a thickness of 120 nm and a second section with a thickness of 140 nm (120 nm of TiO_2 and 20 nm of SnO_2). Each section is responsible for generating a first order LMR with TM polarized light (LMR_{TM}). TiO_2 is deposited by atomic layer deposition (ALD) and SnO_2 by electron-beam deposition. Theoretical results show that the depth of each of the resonances of the dual LMR depends on the length of the corresponding section. Two experimental devices were fabricated with sections of different lengths and their sensitivities studied, achieving values ~4000 nm/RIU with a maximum of 4506 nm/RIU for values of the SRI between 1.3327 and 1.3485.

One of the main concerns in the field of optical sensors is the development of platforms that allow the simultaneous detection of several parameters [1–3], such as temperature, relative humidity, refractive index, etc. This matter also extents to the biosensing field [4–6], where the detection of multiple biomarkers can improve considerably the accuracy in the diagnosis or monitoring of a disease [7–9].

Among optical sensors, Lossy Mode Resonances (LMR) stand out as a high sensitivity refractometric platform [10,11]; which enables their use for biosensing applications [12–15]. LMRs are based on light coupling due to the deposition of a thin-film on a dielectric medium. It occurs when the real part of the thin-film permittivity is positive and greater in absolute value than its own imaginary part and the real part of the permittivity of the waveguide, so metallic oxides and polymers can be employed to generate these resonances [16]. In addition to this, LMRs can be obtained with both transverse electric (TE) and transverse magnetic (TM) polarization [17].

Multiple LMRs can be generated in the same optical spectrum [18]. Nevertheless, as these resonances are generated by the same thin film, their shift is not independent. As a result, sensors with several reference points or LMRs can be obtained using a single device, but they can only be used for sensing a single parameter or analyte.

This problem can be solved in the case of glass slides or coverslips by using both sides of the waveguide, as in [19], where two first order resonances with TE and TM polarization are obtained on each face of the waveguide by depositing the corresponding thin film. A dual sensor for temperature and humidity was manufactured based on this structure by employing polydimethylsiloxane and agarose coatings, respectively.

However, this solution is not possible in the case of a D-shaped optical fiber, where the flat surface of the D-shaped zone is the only part available for deposition. Consequently, the solution must consist of a nanostructure with different thicknesses. The utilization of different coating thicknesses takes advantage of the property of the LMRs to progressively redshift the resonance position in the spectrum by increasing the thickness of the thin film [20].

In this work, a proof of concept step shaped nanostructure was fabricated on the flat surface of a D-shaped optical fiber. This nanostructure enables to obtain for the first time two first order LMRs generated by TM polarization in the same D-shaped optical fiber, and the sensitivity of the resulting devices was studied. The theoretical simulations are supported by experimental results.

D-shaped fibers (purchased from Phoenix Photonics LTD) consist of standard single mode fibers (Corning® SMF-28) with a cladding/core diameter of 125/8 μm and a polished length of 1 cm. These fibers are polished until obtaining an attenuation peak of 0.5 dB at 1550 nm in high refractive index oil (RI = 1.5).

A first thin film of 120 nm of titanium dioxide (TiO_2) is deposited onto the D-shaped zone (length of 10 mm) using the atomic layer deposition (ALD) technique with the Savannah G2 ALD System from Veeco Inc. Then, the D-shaped zone is partially covered using a mask. The mask is placed so approximately half of the D-shaped zone is covered (5 mm) and the other half (5 mm) remains uncovered. A tin oxide (SnO_2) coating with a thickness of 20 nm is fabricated onto the D-shaped optical fiber by electron-beam

deposition with the Nexdep physical vapor deposition platform from Angstrom Engineering Inc. The directionality of the electron beam deposition guarantees that SnO_2 is not deposited on the part of the D-shaped fiber that is covered.

After the second deposition, the mask is removed, therefore obtaining a nanostructure with a step shaped profile. The first section has a thickness of 120 nm of TiO_2, as the SnO_2 was deposited over the mask and it has been removed with it. The second section has a total thickness of 140 nm, the first 120 nm of TiO_2 and the remaining 20 nm of SnO_2. A schematic representation of the resulting structure can be observed in Fig. 1.

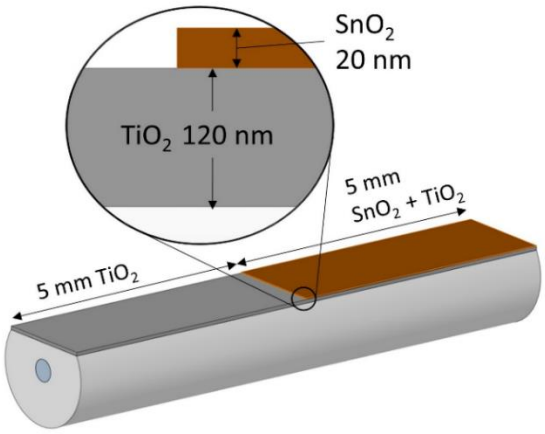

Fig. 1. Schematic representation of the obtained step shaped nanostructure with TiO_2 and SnO_2 on the D-shaped fiber. Dimensions are not to scale.

These thicknesses for both sections were selected with the help of simulations carried out with FIMMWAVE. They were chosen in order to obtain two first order LMR_{TM} close enough so they could be seen in the range of interest but far enough from each other so they did not overlap and could be clearly distinguished.

The refractive index of TiO_2 employed in the theoretical simulations was measured with an ellipsometer UVISEL 2 from Horiba Ltd. (n = 2.619 at 1250 nm, n = 2.16 at 1650 nm) while the extinction coefficient was set to 0.01 to fit the experimental results. It must be considered that the angle of incidence of the ellipsometer required to accurately measure the refractive index does not provide precise results for the extinction coefficient. In the case of SnO_2, a refractive index of 1.9 + 0.01i was used, as in [21], based on ellipsometric measurements performed in [22].

The theoretical results for the previous nanostructure are shown in Fig. 2. Two first order LMR_{TM} can be observed. The resonance that is located at lower wavelengths (that will be called blue LMR from here on) corresponds to the section with a thickness of 120 nm of TiO_2 whereas the LMR that appears at higher wavelengths (that will be called red LMR from now on) corresponds to the section with a thickness of 140 nm (120 nm TiO_2 + 20 nm SnO_2). For the sake of simplicity, the combination of the blue LMR and the red LMR will be referred as dual LMR.

In the measuring setup, one end of the D-shaped optical fiber is connected to a broadband multi-SLED light source (FJORD-X3-1330-1650 from Pyroistech S.L.) through an in-line polarizer and a polarization controller (Phoenix Photonics Ltd), which enable selecting the TE- or TM-polarized state of light [22]. Once the polarization state has been adjusted, the fiber is fixed so the polarization state does not change. The other end is connected to an optical spectrum analyser (MS9740A from Anritsu) to observe the resonance in the 1250-1700 nm range while the D-shaped zone is immersed in ultrapure water (18.1 MΩ/cm).

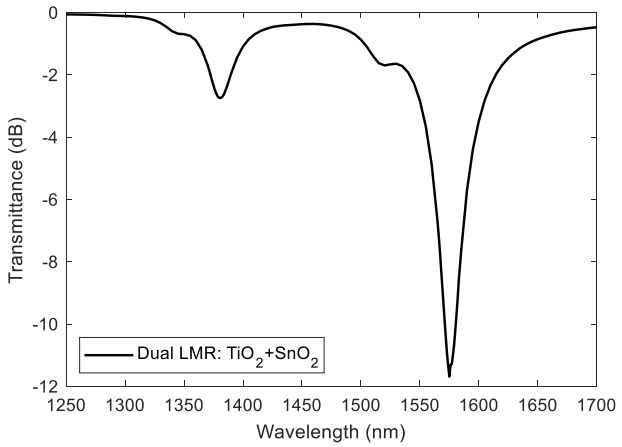

Fig. 2. Theoretical results for a dual LMR obtained with a first section 5 mm long with a thickness of 120 nm of TiO_2 and a second section 5 mm long with a thickness of 120 nm of TiO_2 and 20 nm of SnO_2 on a D-shaped SMF.

In Fig. 3, corresponding to the experimental results, the initial LMR (120 nm of TiO_2 over a length of 10 mm) and the final dual LMR can be observed. The dual LMR resembles the theoretical simulation in Fig. 2. The appearance of two clearly distinguishable resonances indicates that the thickness difference between the two sections is far greater than the non-uniformities in each section, fact corroborated by the simulations. If there were high non-uniformities, both resonances would overlap. Regarding the thickness change from one section to the other, neither experimentally nor theoretically, any edge effects have been observed. The tapered ends of the D-shaped region do not have either a high impact in the resonances [21].

In order to demonstrate the independence of both resonances of the dual LMR, each of them is shown separately. To achieve these results, the part of the D-shaped zone that corresponds to each LMR was immersed in ultrapure water while the rest of the device was left in air, obtaining only the desired resonance. It can be observed that the dual LMR is equal to the addition of the blue and red LMRs.

The blue LMR (corresponding to 5 mm with a thickness of 120 nm of TiO_2) is located next to the initial LMR since both have the same thickness. The slight displacement may be due to oxidation of the material or the deposition of some SnO_2 under the mask. The blue LMR is not as deep as the original LMR with a thickness of 120 nm due to its shorter deposition length (5 mm instead of 10 mm)

The red LMR of the final structure has undergone a redshift due to the greater thickness of deposited material. The red LMR has a greater depth than the blue LMR, because with the same deposited length, the further towards the red the LMR is, the greater its depth.

The sensitivity of the device to the surrounding medium refractive index (SRI) for values close to water has also been studied, considering its interest for biosensing applications.

The setup is the same as the one that has been previously explained, but in this case the D-shaped region is placed inside a microfluidic system that is thermo-stabilized to 26ºC by means of two Peltier cells, as in [13]. The microfluidic system consists of two equal-size pieces, the upper one is made of ULTEM® and the lower

one is made of stainless steel. A microfluidic channel is engraved on both bars with dimensions 1 mm × 1 mm × 50 mm (volume of 50 µL), with the D-shaped region fitting in this channel. A peristaltic pump allows to control the flow through the cell.

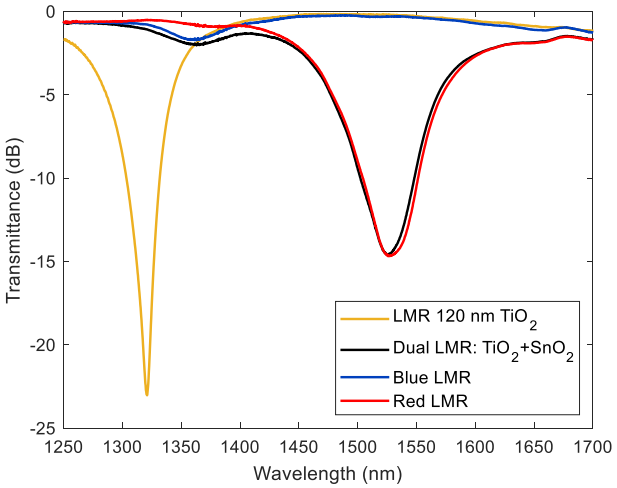

Fig. 3. Experimental results for a dual LMR obtained with a first section 5 mm long with a thickness of 120 nm of TiO_2 and a second section 5 mm long with a thickness of 120 nm of TiO_2 and 20 nm of SnO_2 on a D-shaped SMF.

The device response has been monitored with five refractive indices, as shown in Fig. 4. The first of them corresponds to ultrapure water and the remaining four correspond to solutions of glucose in ultrapure water with refractive indices of 1.3327, 1.3371, 1.3412, 1.3448 and 1.3485 respectively, measured with refractometer Refracto30GS from Mettler Toledo Inc. The sensitivity values obtained are 4048 nm/RIU in the case of the blue LMR and 3914 nm/RIU in the case of the red LMR, with a figure of merit (FOM) of 58 RIU^{-1} for the latter resonance (full width half maximum, FWHM, of 68 nm). These sensitivities are near the typical values for LMR based sensors, which are around 5000 nm/RIU [13]. It can also be observed that the resonances widen as they shift towards the red, as it is mentioned in the literature [22].

The operation principle of LMR-based sensors consist of resonance wavelength or maximum power attenuation tracking. Nevertheless, in the previous device, the blue LMR is not very well defined (depth of only -2.0 dB) in comparison with the red LMR (depth of -14.6 dB) which can difficult its monitoring. In consequence, it would be interesting for this type of devices that both resonances had the same depth or at least, if the resonances were different, that they had a minimum depth of -5 dB or more. Here, it has to be considered that the depth of the LMR increases at longer wavelengths and with the length of the D-shaped fiber [10].

Therefore, in order to obtain a twin LMR where the blue and the red LMR have similar depths, it has been decided to modify the length of each section. A new device is manufactured where the covered section of the D-shaped zone (final thickness of 120 nm) is around 7.5 mm while the uncovered section (final thickness of 140 nm) is approximately 2.5 mm.

Fig. 5 shows the theoretical results for different lengths of the first (120 nm thick) and the second (140 nm thick) sections. If we compare Fig. 2 and Fig. 5 it can be appreciated that when both sections measure 5 mm, the theoretical depths of the blue and the red LMR are -2.7 dB and -11.7 dB respectively whereas for the lengths of 7.5 and 2.5 mm, the depths are very similar (-10.7 dB and -9.3 dB respectively), which is the desired result.

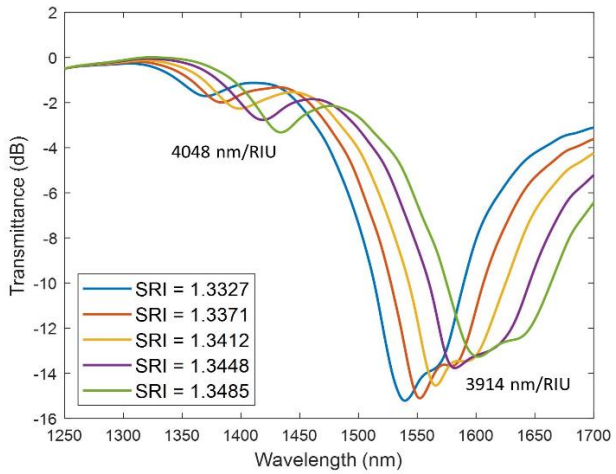

Fig. 4. Experimental sensitivity of the blue and the red LMR of the first device for five refractive indices.

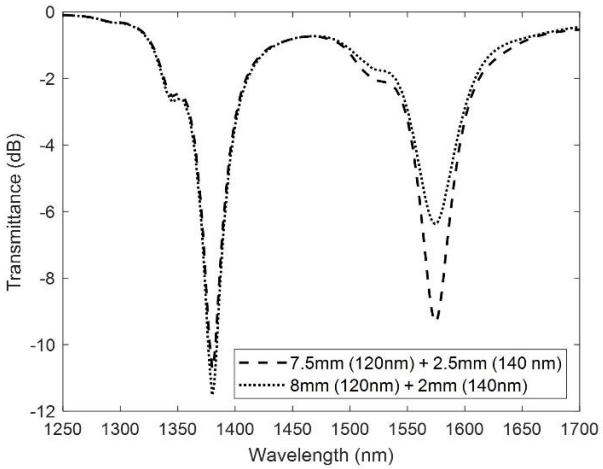

Fig. 5. Theoretical results for a dual LMR obtained with different lengths for the first section (thickness of 120 nm of TiO_2) and the second section (thickness of 120 nm of TiO_2 and 20 nm of SnO_2) on a D-shaped SMF.

In Fig. 6, the initial LMR and the final twin LMR are shown for this new device. In this case, the blue LMR reaches -13.8 dB while the red LMR achieves -6.3 dB. Comparing Fig. 6 with the theoretical simulations in Fig. 5, it seems that approximately, 8 mm of the D-shaped zone remained covered (final thickness of 120 nm) while 2 mm stayed uncovered (final thickness of 140 nm) instead of the initially planned 7.5/2.5 mm proportion.

On the other hand, both the red and blue LMR are shown separately in Fig. 6, and it can be checked that the twin LMR is the addition of both. It is also worth mentioning that the position of the blue LMR has slightly shifted compared to the position of the initial LMR (120 nm thickness along 10 mm), as it happened in the first device. In this case, the depth of the blue LMR is very similar to the

depth of the initial LMR, which is coherent with the fact that most of the D-shaped zone has been covered during the second deposition.

Finally, the sensitivity has also been studied for this second device with the previous five refractive indices, achieving 3977 nm/RIU in the case of the blue LMR and 4506 nm/RIU for the red one, as it can be observed in Fig. 7. The sensitivity is higher for the resonance located at a longer wavelength, as expected [22]. The FOM is respectively 126 RIU^{-1} for the shorter wavelength resonance and 35 RIU^{-1} for the longer wavelength one.

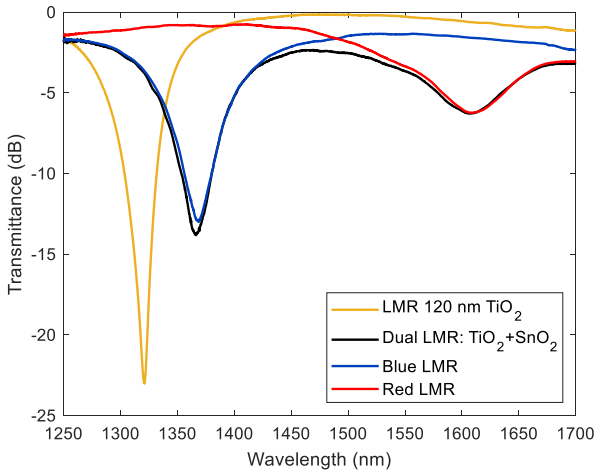

Fig. 6. Experimental results for a dual LMR obtained with a first section 8 mm long with a thickness of 120 nm of TiO_2 and a second section 2 mm long with a thickness of 120 nm of TiO_2 and 20 nm of SnO_2 on a D-shaped SMF.

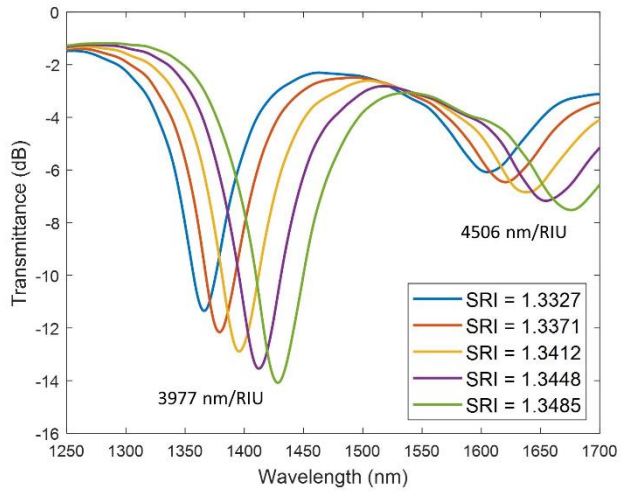

Fig. 7. Experimental sensitivity of the blue and the red LMR of the second device for five refractive indices.

In this Letter, a proof of concept nanostructure with two sections of different thickness fabricated on a D-shaped optical fiber was validated to obtain two independent LMRs. This means that each resonance only shifts when the SRI in which the corresponding section of the D-shaped fiber is immersed varies. To our knowledge, this is the first time that two independent LMRs are obtained in the same D-shaped optical fiber. It was also demonstrated, both theoretically and experimentally, that the depth of each of the resonances of the dual LMR depends on the length of the D-shaped section that generates it. Finally, the sensitivity of the obtained devices was also studied, reaching values ~4000 nm/RIU with a maximum of 4506 nm/RIU for values of the SRI between 1.3327 and 1.3485.

These results open the door for the development of applications where each resonance can be made sensitive to a different parameter or analyte of interest therefore obtaining multi-parameter sensors, including biosensors for the detection of several biomarkers.

Funding. The authors would like to acknowledge the Spanish Ministry of Universities the support of this work through FPU18/03087 grant (Formación de Profesorado Universitario) and to the Spanish Ministry of Science and Innovation PID2019-106231RB-I00 TEC Research fund.

Disclosures. The authors declare no conflict of interest.

References

1. J. Hromadka, S. Korposh, M. C. Partridge, S. W. James, F. Davis, D. Crump, and R. P. Tatam, Sensors Actuators, B Chem. **244**, 217 (2017).
2. S. Pevec and D. Donlagic, IEEE Photonics J. **9**, (2017).
3. H. T. Kim and M. Yu, Sci. Rep. **9**, 1 (2019).
4. A. L. Washburn, M. S. Luchansky, A. L. Bowman, and R. C. Bailey, Anal. Chem. **82**, 69 (2010).
5. R. Huang, Y. Liao, X. Zhou, Y. Fu, and D. Xing, Sensors Actuators, B Chem. **247**, 505 (2017).
6. Z. Liao, Y. Zhang, Y. Li, Y. Miao, S. Gao, F. Lin, Y. Deng, and L. Geng, Biosens. Bioelectron. **126**, 697 (2019).
7. T. Muinao, H. P. Deka Boruah, and M. Pal, Heliyon **5**, e02826 (2019).
8. T. Nozaki, S. Sugiyama, H. Koga, K. Sugamura, K. Ohba, Y. Matsuzawa, H. Sumida, K. Matsui, H. Jinnouchi, and H. Ogawa, J. Am. Coll. Cardiol. **54**, 601 (2009).
9. S. F. Shariat, P. I. Karakiewicz, R. Ashfaq, S. P. Lerner, G. S. Palapattu, R. J. Cote, A. I. Sagalowsky, and Y. Lotan, Cancer **112**, 315 (2008).
10. F. J. Arregui, I. Del Villar, C. R. Zamarreño, P. Zubiate, and I. R. Matias, Sensors Actuators, B Chem. **232**, 660 (2016).
11. A. Ozcariz, C. R. Zamarreño, P. Zubiate, and F. J. Arregui, Sci. Rep. **7**, 1 (2017).
12. P. Zubiate, C. R. Zamarreño, P. Sánchez, I. R. Matias, and F. J. Arregui, Biosens. Bioelectron. **93**, 176 (2017).
13. P. Zubiate, A. Urrutia, C. R. Zamarreño, J. Egea-Urra, J. Fernández-Irigoyen, A. Giannetti, F. Baldini, S. Díaz, I. R. Matias, F. J. Arregui, E. Santamaría, F. Chiavaioli, and I. Del Villar, (2019).
14. J. J. Imas, C. Ruiz Zamarreño, P. Zubiate, J. Campión, L. Sánchez-Martín, and I. R. Matías, in *IEEE Sensors 2020* (2020).
15. A. B. Socorro, J. M. Corres, I. Del Villar, F. J. Arregui, and I. R. Matias, Sensors Actuators, B Chem. **174**, 263 (2012).
16. I. Del Villar, F. J. Arregui, C. R. Zamarreño, J. M. Corres, C. Bariain, J. Goicoechea, C. Elosua, M. Hernaez, P. J. Rivero, A. B. Socorro, A. Urrutia, P. Sanchez, P. Zubiate, D. Lopez, N. De Acha, J. Ascorbe, and I. R. Matias, Sensors Actuators, B Chem. **240**, 174 (2017).
17. C. Ruiz Zamarreño, P. Zubiate, M. Sagües, I. R. Matias, and F. J. Arregui, Opt. Lett. **38**, 2481 (2013).
18. C. R. Zamarreño, F. J. Arregui, I. Del Villar, I. R. Matias, and M. Hernaez, J. Light. Technol. Vol. 28, Issue 1, pp. 111-117 **28**, 111 (2010).
19. I. Dominguez, I. Del Villar, O. Fuentes, J. M. Corres, and I. R. Matias, Sci. Rep. **11**, 3669 (2021).
20. I. Del Villar, M. Hernaez, C. R. Zamarreno, P. Sánchez, C. Fernández-Valdivielso, F. J. Arregui, and I. R. Matias, Appl. Opt. **51**, 4298 (2012).
21. O. Fuentes, P. Vaiano, I. del Villar, G. Quero, J. Corres, M. Consales, I. Matías, and A. Cusano, Opt. Lett. **45**, 4738 (2020).
22. F. Chiavaioli, P. Zubiate, I. Del Villar, C. R. Zamarreìo, A. Giannetti, S. Tombelli, C. Trono, F. J. Arregui, I. R. Matias, and F. Baldini, ACS Sensors **3**, 936 (2018).